



Heterometallic [Ln(hfac)₃Cu(acac)₂] complexes with late 4f ions

Luca Bellucci^a, Luca Giordano^a, Silvia Carlotto^{b,c}, Giordano Poneti^{d,1}, Marzio Rancan^b,
Simona Samaritani^a, Lidia Armelao^{c,e}, Luca Labella^{a,*}

^a Dipartimento di Chimica e Chimica Industriale and CIRCC, Università di Pisa, via Giuseppe Moruzzi 13, I-56124 Pisa, Italy

^b CNR ICMATE and INSTM, c/o Dipartimento di Scienze Chimiche, Università di Padova, via Marzolo 1, I-35131 Padova, Italy

^c Dipartimento di Scienze Chimiche and CIRCC, Università di Padova, via Marzolo 1, I-35131 Padova, Italy

^d Instituto de Química, Universidade Federal do Rio de Janeiro, Avenida Athos da Silveira Ramos, 149, Centro de Tecnologia – Cidade Universitária, 21941-909, Rio de Janeiro, Brazil

^e CNR DSCTM, Piazzale A. Moro 7, 00185 Roma, Italy

ARTICLE INFO

Dedicated to Professor Guido Pampaloni on the occasion of his retirement, for his contribution to inorganic chemistry

Keywords:

Heterometallic *d-f* complexes

Lanthanide metals

Dysprosium

Magnetisation dynamics

Phonon bottleneck effect

ABSTRACT

Heterometallic [Ln(hfac)₃Cu(acac)₂] complexes (Ln = Eu **1**, Dy **2**, Er **3**) can be prepared along the *f*-transition series. X-rays diffraction studies on well-shaped single crystals revealed for **1** – **3** a dinuclear structure. No ligand scrambling occurred, a Lewis acid-base interaction has been observed with the two metals bridged through two oxygen atoms of the acetylacetonato ligands and an oxygen atom of a hexafluoroacetylacetonato ligand. Compounds **2** and **3** can be obtained only in anhydrous conditions. (**1**) can be sublimed under reduced pressure, and crystals of the sublimed product, **1a**, showed a polymorph structure with the same molecular identity. Magnetic studies have been carried out on **2**, displaying an antiferromagnetic interaction and a field-induced slow relaxing magnetic moment with a significant phonon bottleneck effect. Compound **3**, on the other hand, did not present any magnetization dynamics, with or without applied field. Quantum mechanical calculations rationalize the variation of the bond strengths from the reagents to the heterometallic complexes and quantify the Ln and Cu direct interaction, which is relevant, especially for **2**.

1. Introduction

The synthesis of heterometallic complexes involving 3d and 4f metal ions is currently of great interest for potential applications in various research fields for their luminescence, catalytic and magnetic properties [1]. From the magnetic point of view, polymetallic lanthanide-based coordination systems have been frequently used to reduce the tunneling of the magnetization in zero applied magnetic field, in order to slow down the magnetization dynamics and increase the magnetic relaxation time [2], as candidates for spin-based quantum bits [3], or to prepare multifunctional molecular materials combining luminescence [4] or ferroelectricity [5] with magnetism.

The synthetic strategies used to prepare heterometallic lanthanide systems often rely on the different affinity of 3d-4f metals towards nitrogen and oxygen donor ligands [6]. The rational design of heterotopic linkers, multidentate ligands with different binding sites, can afford heterometallic discrete molecular complexes as well as coordination polymers [7,2d]. Since it is normally difficult to control the synthesis for

lanthanide lability and for lanthanide tendency to high and variable coordination geometries, rigid, often complicate, multidentate ligands able to minimize ligands scrambling reactions are often chosen [8]. Different synthetic approaches exploiting a metallo-ligand precursor or a simple self-assembly route have in common the pivotal role of the hypodentate ligand or of the connector to selectively drive the synthesis to a pure heterometallic compound rather than a mixture of products.

On the other hand, many reports in the literature describe the tendency of a rare-earth ion to expand the coordination sphere of a formally unsaturated mononuclear tris β -diketonato lanthanide fragment with one or two additional neutral ligands, acting as Lewis bases, in order to get typically a coordination number eight or nine [9]. Hexafluoroacetylacetonato (hfac) ligands, presenting a high electron withdrawing ability, favour in fact reactions of a formally unsaturated fragment even with low-basicity donors. Numerous heterometallic *d-f* complexes can be formed by adduct formation between a rare-earth tris β -diketonate and a transition metal complex [10,7b]. Most of such examples report Schiff-base dianionic ligands with two binding sites, a

* Corresponding author.

E-mail address: luca.labella@unipi.it (L. Labella).

¹ Current address: Dipartimento di Scienze Ecologiche e Biologiche, Università degli Studi della Tuscia, Largo dell'Università, 01100, Viterbo, Italy.

N_2O_2 donor set typically used for dipositive *d*-transition metals with two oxygen atoms usually from phenolate groups saturating the coordination sphere of a β -diketonate lanthanide fragment [11]. Msalen ($M = 3d$; salen = *N,N'*-ethylenebis(salicylideneaminato)) species have excess charge density on the oxygen atoms and favour the formation of stable heterometallic $[\text{M}(\text{salen})\text{RE}(\text{hfac})_3]$ complexes along the lanthanide series. Many complexes with salen-type ligands have been used to synthesise *d-f* heterometallic complexes [12]. Research in the field has been orientated by the pioneering work of Gatteschi and co-workers [13] which revealed a ferromagnetic coupling between copper(II) and gadolinium(III) in a molecular architecture with the two cations in close proximity.

Lanthanides share prevalently electrostatic chemistry, where the major difference is the ionic radius decreasing along the series, therefore isostructural families of compounds for all 4f metals are not uncommon [14]. Structural discontinuity has been normally observed for early-transition elements where the differences in the ionic radius for close elements are larger [15]. A heterometallic $[\text{Cu}(\text{acac})_2\text{Ln}(\text{hfac})_3]$ dinuclear compound has been reported for lanthanum where the oxygen atoms of a β -acetylacetonate copper(II) fragment resulted to have sufficient basicity to bind $\text{La}(\text{hfac})_3$ [16], nevertheless, this result was not obtained with rare-earth ions of smaller ionic radius. For both yttrium [17] and dysprosium [18], $[\text{RE}(\text{hfac})_3(\text{H}_2\text{O})_2]$ have been reported to co-crystallize with copper(II) acetylacetonate, yielding $[\text{RE}(\text{hfac})_3(\text{H}_2\text{O})_2][\text{Cu}(\text{acac})_2]$ where $[\text{RE}(\text{hfac})_3(\text{H}_2\text{O})_2]$ and $[\text{Cu}(\text{acac})_2]$ molecules are linked by intermolecular hydrogen bonds, not forming a genuine heterometallic complex. Since the rare-earth complexes of the type $[\text{RE}(\text{hfac})_3]$, $[\text{RE}(\text{fod})_3]$ and $[\text{RE}(\text{pta})_3]$ were found to form heterometallic complexes with $[\text{Cu}(\text{acacen})]$ or $[\text{Ni}(\text{acacen})]$, (where H_2acacen is *N,N*-ethylenebis(acetylacetonimine) [19], Hfod is 6,6,7,7,8,8,8-heptafluoro-2,2-dimethyl-3,5-octanedione and Hpta is pivaloyltrifluoroacetone), also for late *f*-transition metals, a lower basicity of the oxygen atoms of acetylacetonate ligands in the copper compound with respect to the ones of the Schiff-base copper complexes can be inferred [16]. The resulting binuclear complexes sublimed without decomposition at temperatures of 200–240 °C at 0.01 mm Hg, showing promise for investigation of magnetic properties of thin films prepared through chemical vapor deposition [20]. This synthetic approach, leading to stable Lewis acid/Lewis base adducts, has also been exploited for tripositive *d*-transition metals by Lindoy et al. in the synthesis of $[\text{Eu}(\text{fod})_3\text{Co}(\text{acac})_3]$ [21]. Studies in solution have as well identified the heterometallic complex formation [22]. Moreover, the coordinating properties of the solvents have been shown to be important in the determination of the structure of the final 3d-4f adduct, as pointed out by a recent contribution from Bendix and Perfetti [23], reporting facially-coordinated $[\text{LnM}(\text{hfac})_3(\mu_2\text{-acac-O,O'})_3]$ ($\text{Ln} = \text{La, Pr, Gd}$; $\text{M} = \text{Cr, Fe, Ga}$) systems prepared in a non-coordinating medium (benzene). This synthetic route has been shown to be quite versatile, affording access to heterobimetallic complexes for different lanthanide centers, tripositive metals and oxygen donor chelate ligands. Following this synthetic approach, heterometallic complexes $[\text{Ln}(\text{hfac})_3\text{Al}(\text{LL}')_3]$ (with $\text{Ln} = \text{Eu, Tb, Gd}$ and $\text{HLL}' = \text{methyl acetoacetate, salicylaldehyde, 2-hydroxynaphthaldehyde}$) with tunable luminescence properties can be prepared [24].

In this context, being highly interested in the study of discontinuities of the properties along the lanthanide series, the literature statement [16] “for elements of the middle and the end of lanthanide series such as Gd, Lu and Y, formation of $[\text{Ln}(\text{hfac})_3\text{Cu}(\text{acac})_2]$ is most probably impossible” has attracted our attention and has directed new synthetic efforts on middle to late lanthanide-copper compounds. In this work, we show that for the synthesis of heterometallic dinuclear complexes $[\text{Ln}(\text{hfac})_3\text{Cu}(\text{acac})_2]$, this approach holds not only for lanthanum or early-lanthanide metals but also for smaller Ln(III) ions ($\text{Ln} = \text{Eu, Dy, Er}$). Access to late *f*-transition metal heterobimetallic complexes only occurs in anhydrous conditions.

2. Result and discussion

Reacting $[\text{Eu}(\text{hfac})_3(\text{H}_2\text{O})_2]$ with $[\text{Cu}(\text{acac})_2]$ in DCE at 60 °C in a molar ratio 1:1 a single product has been recovered. Elementary data on the crude product support the formation of an adduct between the two building blocks. The IR spectrum closely looks like, in the 1700–650 cm^{-1} range, the spectrum of $[\text{La}(\text{hfac})_3(\text{H}_2\text{O})\text{Cu}(\text{acac})_2]$ prepared for comparison purposes, Figure S1. The two spectra differ in the presence of large water absorption. The europium compound does not absorb water for short term air expositions. Well-shaped crystals are suitable for an X-ray diffraction study have been recovered from a hot heptane solution. The molecular structure of the heterobimetallic compound is shown in Fig. 1.

Compound $[\text{Eu}(\text{hfac})_3\text{Cu}(\text{acac})_2]$ (1) crystallizes in the $P2_1/n$ space group. Europium is eight-coordinated by 6 oxygen atoms of three hfac ligands and 2 oxygen atoms (O7 and O8) of two acac ligands. A stereochemical study of the Eu centre based on a continuous shape measures (CSHMs) analysis has been performed with the SHAPE 2.1 software, considering an eight-coordination [25], showing that Eu coordination geometry is very close to an ideal triangular dodecahedron (TDD-8, Table S1). Copper displays a marked preference for pentacoordination, presenting a distorted square pyramidal geometry arising from an oxygen atom from a hfac (O4) and 4 oxygen atoms from two acac ligands. A hfac ligand with an oxygen atom bridging 3d-4f metal centres has only few precedents in the literature [26]. The bridging oxygen atoms display longer metal–oxygen distances: while Eu1–O4, Eu1–O7 and Eu1–O8 have lengths in the range 2.438–2.508 Å, the other Eu–O distances span the 2.336–2.381 Å range. Cu1–O4 length is 2.416 Å while the other Cu–O distances are much shorter (in the range 1.897–1.966 Å). The intermetallic distance Eu1–Cu1 is 3.306 Å, and the closest Eu–Eu distance is 8.767 Å. One of the six members ring “ CuO_2C_3 ” of the coordinated acac ligand shows stacking interactions resulting in supramolecular dimers (Fig. 1), elsewhere reported in the literature [27]. The centroid–centroid distance between the stacking fragments is 3.229 Å.

$[\text{Eu}(\text{hfac})_3\text{Cu}(\text{acac})_2]$ is an air stable heterobimetallic complex, well soluble in common organic solvents, sublimable in mild conditions (10^{-2} mbar at 110 °C). Actually, the sublimed product 1a has a slightly different IR spectrum (Figure S2). Bands at 1614 and 1585 cm^{-1} present in 1 are here absent, while new bands at 1558 and 1288 cm^{-1} and small differences in the relative intensities are present. IR spectra show no changes on prolonged air exposition. The sublimed product has been recrystallized from heptane and a structural study through single crystal X-ray diffraction has clarified that the molecular identity is maintained although in a different polymorphic phase (*P*-1 space group), having two independent molecules in the unit cell, Figure S5.

The main difference in the molecular structure of the two independent molecules of the sublimed product is in the distance of Cu–O_{hfac} (2.416 Å for 1, and 2.5515; 2.532 Å for the sublimated 1a). An overlay between 1 and 1a structures is reported in Fig. 2. CSHMs analysis for 1a shows that the two Eu centres have a coordination geometry closer to a square antiprism (SAPR-8, Table S1). Finally, also in this case, each of the two crystallographic independent molecules forms supramolecular dimers due to stacking between “ CuO_2C_3 ” fragments (centroid–centroid distances 3.114 and 3.324 Å).

The heterometallic *d-f* compound $[\text{Eu}(\text{hfac})_3\text{Cu}(\text{acac})_2]$ in 1 and 1a, closely resembling the hydrated lanthanum compound,¹⁶ is formally described as the product of a Lewis acid-base reaction exploiting the ability of the “ $\text{Eu}(\text{hfac})_3$ ” fragment to expand its coordination sphere. The coordination number 8 of europium is the main difference with respect to the lanthanum analogue, easy to rationalize for the significant lower ionic radius of europium. No exchange of ligands has been noticed.

The synthetic procedure can be repeated for dysprosium and erbium, a late *f*-transition element with an ionic radius smaller than yttrium. Starting from equimolar amounts of $[\text{Ln}(\text{hfac})_3(\text{H}_2\text{O})_2]$ ($\text{Ln} = \text{Dy, Er}$)

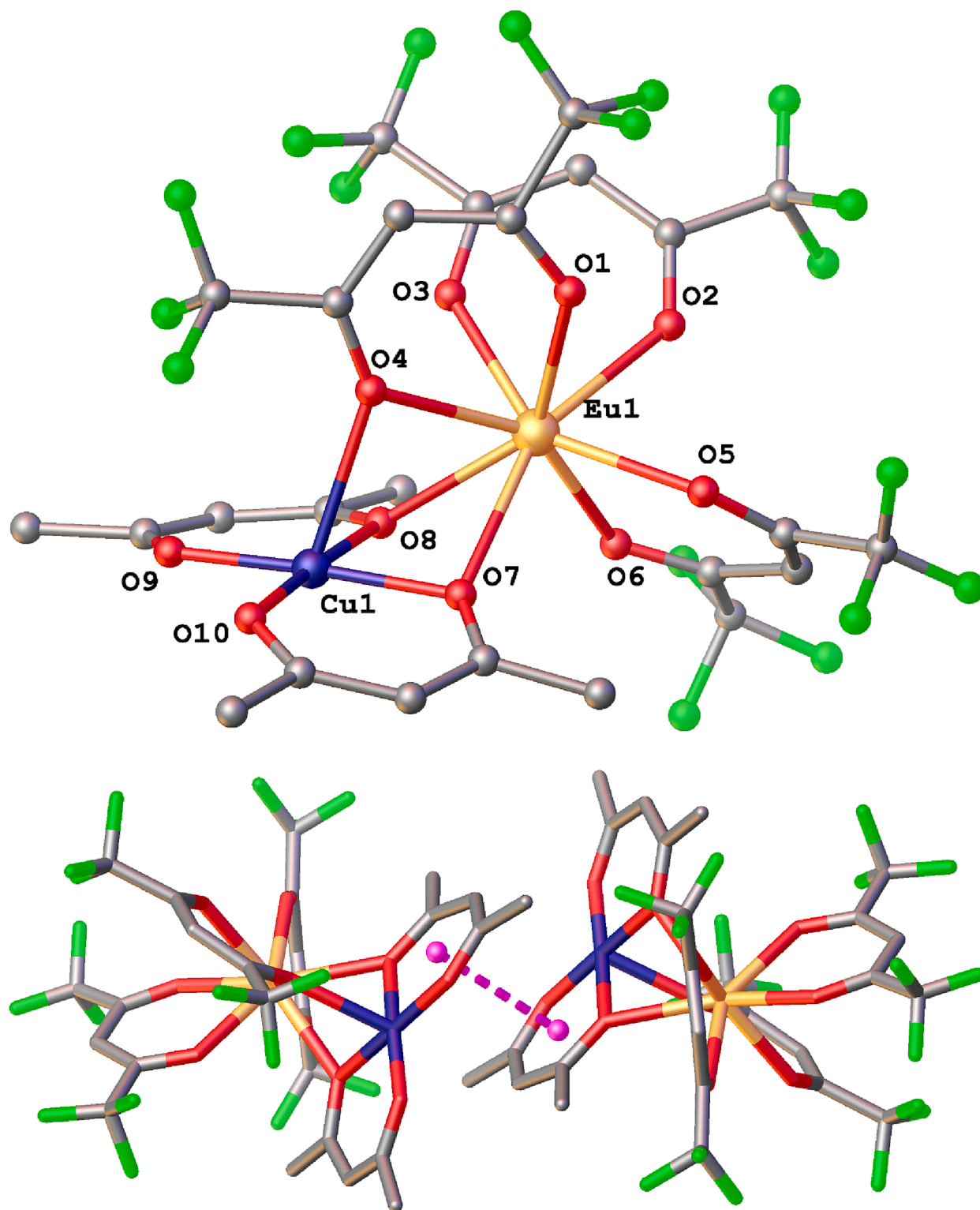


Fig. 1. Molecular structure of $[\text{Eu}(\text{hfac})_3\text{Cu}(\text{acac})_2]$ in **1** and supramolecular dimer due to “ CuO_2C_3 ” fragments stacking. Color code: C, gray; O, red; F, green; Cu, blue; Eu, light orange; centroid, purple. H atoms and disordered parts omitted for clarity. (For interpretation of the references to color in this figure legend, the reader is referred to the web version of this article.)

and $[\text{Cu}(\text{acac})_2]$ in DCE at 60°C a light violet solution has been obtained. The products have been recovered after anhydrication with P_4O_{10} of the residues obtained removing the volatile phase from the reaction mixtures. Analytical data are in good agreement with the composition $[\text{Ln}(\text{hfac})_3\text{Cu}(\text{acac})_2]$. The IR spectra closely resemble that of $[\text{Eu}(\text{hfac})_3\text{Cu}(\text{acac})_2]$ (Figure S3), although they are changing with

time for air exposition. For instance, for **3**, bands at 1586 and 1454 cm^{-1} disappear while bands at 1485 , 1289 and 759 cm^{-1} are growing together with a large band in the $3600\text{--}3000$ range, Figure S4. Single crystals of the two compounds **2** and **3** $[\text{Ln}(\text{hfac})_3\text{Cu}(\text{acac})_2]$ ($\text{Ln} = \text{Dy}$ **2**, Er **3**), obtained from a heptane solution at -20°C , have been studied through single crystal X-ray diffraction and found to be isostructural

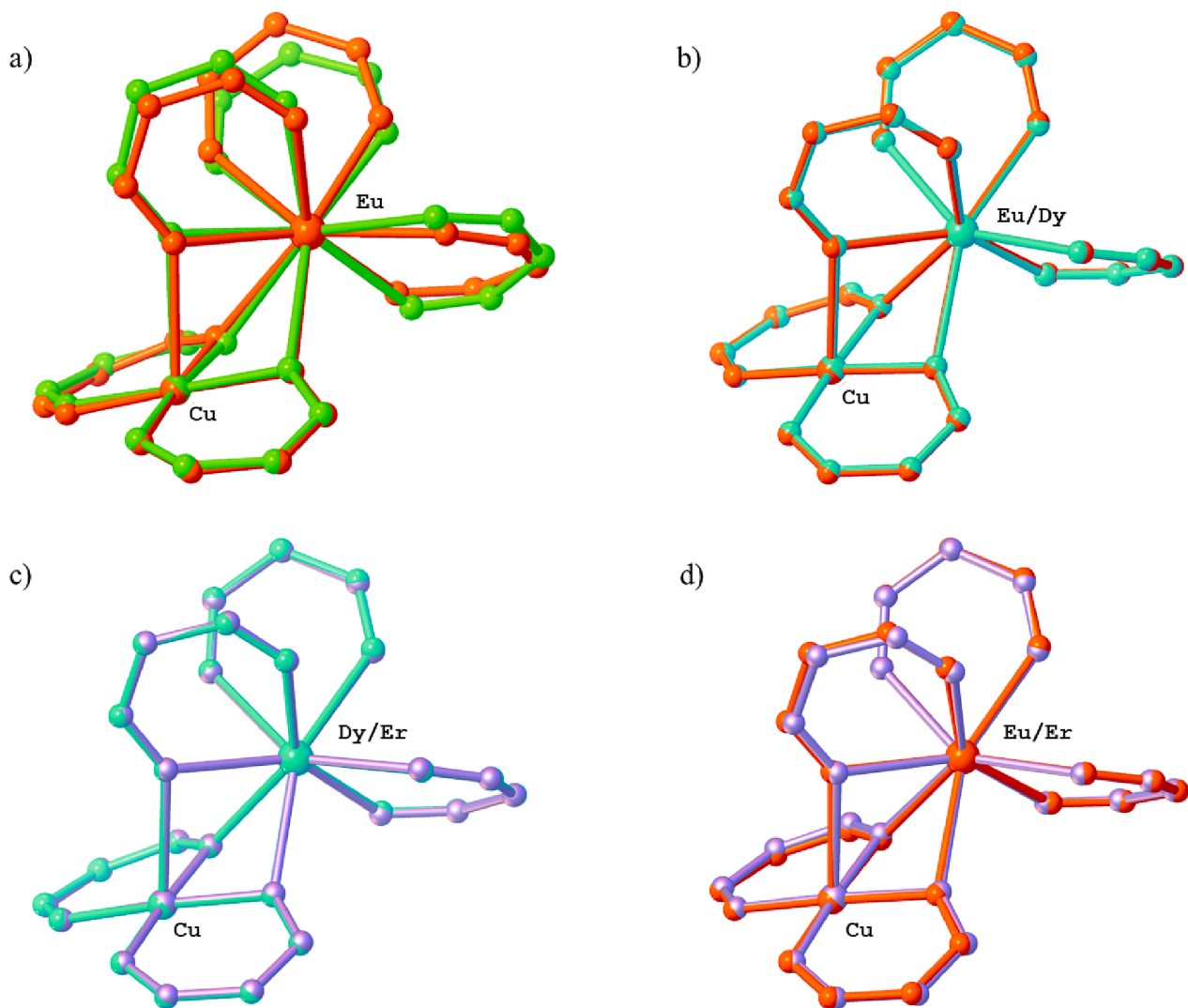


Fig. 2. Overlays between the $[\text{Ln}(\text{hfac})_3\text{Cu}(\text{acac})_2]$ structures. Colour code: red, 1; green, 1a; cyan, 2; purple, 3. Ligands CH_3 and CF_3 groups were removed for clarity. (For interpretation of the references to color in this figure legend, the reader is referred to the web version of this article.)

with the europium analogue **1**, Table S3 and Figures S6 and S7. The $\text{Cu}-\text{O}_{\text{hfac}}$ bond distance is here 2.390 and 2.382 Å, for Dy and Er respectively, slightly shorter than in the europium compounds **1** and **1a** (2.42 Å or 2.53 Å, respectively). Overlays between compounds **1**–**2**, **2**–**3**, and **1**–**3** are reported in Fig. 2. In **2** and **3**, the stacking between “ CuO_2C_3 ” fragments leading to supramolecular dimers have similar distances close to 3.2 Å. For compound **2**, the CShMs analysis suggests a TDD-8 coordination geometry, while, for compound **3**, it gives essentially the same value for both the SAPR-8 and TDD-8 coordination geometries (Table S1). Intermetallic Er-Cu (3.255 Å) and Dy-Cu (3.269 Å) distances are similar to what found in **1** and **1a** and much shorter compared to 5.87 Å found in the co-crystallized product.[14] Crystals of **2** and **3** quickly become amorphous on air exposition being air sensitive also in the solid state. Ligand exchange was observed if sublimation of **3** is carried out in air, yielding the mixed ligand $[\text{Cu}(\text{hfac})(\text{acac})]$ complex, **4**, already reported in the literature [28]. The structure of **4** has been identified in the sublimed product through single crystal X-ray diffraction (Figure S8). These results are consistent with previous observations of a ligand exchange for the co-crystallized $[\text{Y}(\text{hfac})_3(\text{H}_2\text{O})_2][\text{Cu}(\text{acac})_2]$ compound [13] yielding $[\text{Cu}(\text{hfac})_2]$ on heating [29].

2.1. Magnetic study of **2** and **3**

The analysis of the static magnetic properties of compound **2** is reported in Fig. 3. The room temperature value of the $\chi_M T$ product is 14.74 emuK/mol, in line with the theoretical 14.55 value expected for uncoupled Dy(III) and Cu(II) ions. Upon cooling, the $\chi_M T$ product decreases to reach 12.55 emuK/mol at 2.5 K, in line with the depopulation of the m_J levels of the rare earth, split by the crystal field. Below this temperature, there is a steeper decrease of the curve, to reach 12.42 emuK/mol at 2.0 K. This decrease can be attributed to the Dy(III) magnetic anisotropy or to a feeble intramolecular antiferromagnetic interaction between the two ions.

The isothermal magnetization curves of **2** display, at low fields, a rapid increase followed by a pseudo-saturation, with a magnetization reaching the $6.54 \mu_B \cdot \text{mol}^{-1}$ value at 2.0 K and 7 T. The absence of a saturation value, along with the non-overlapping nature of the three curves when reported as a function of the H/T parameter (Figure S10), show that the ground state is not a pure Kramers doublet, but includes contributions from higher energy states. This is not surprising, due to the relatively low symmetry of the first coordination sphere of the Dy(III) ion, previously reported to generate significant mixing among the crystal-field split Kramers doublets [30].

A careful inspection of the plots at low fields shows a stepped-like

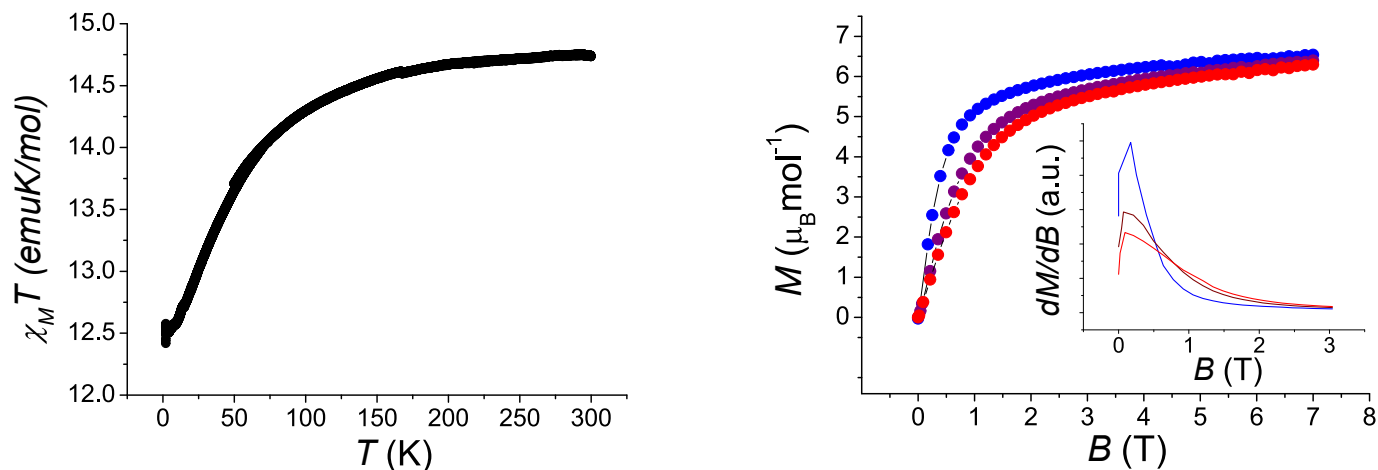


Fig. 3. Left panel: Temperature dependence of the $\chi_M T$ product of **2**. Right panel: Isothermal field dependencies of the magnetic moment of **2** (2 K (blue circles), 4 K (purple circles), 5 K (red circles)). Inset: first derivative of the magnetization curves as function of the magnetic field (same colour code). (For interpretation of the references to color in this figure legend, the reader is referred to the web version of this article.)

increase, highlighted by derivation as a function of the magnetic field (see inset of Fig. 3). The maxima in the differential curves appear in the 0.1–0.16 T range. These changes in the slope of the isothermal magnetization curves suggest the presence of an antiferromagnetic interaction between the Dy(III) and the Cu(II) ion. From the field values of the maxima, its magnitude may be estimated to be lower than 0.15 cm^{-1} . Similar values of the antiferromagnetic interaction constant have been observed previously in others Dy(III)-Cu(II) exchange coupled systems [30b,31]. Antiferromagnetic exchange between Dy(III) and Cu(II), although previously reported [32,10a], is rarer than the ferromagnetic one [33,8a], and it is known to depend on the DyOOCu dihedral angle: the smaller the angle, the more favoured the antiferromagnetic magnetic interaction [10a]. The “switching angle” between ferro- and antiferromagnetic interaction has been reported to be close to 135° , close to the ones found for **2** (134.3° , see Figure S11) [10a]. Pointillart, Ouahab and coworkers reported, for a coupled Dy(III)-Cu(II) heterometallic system with comparable Dy-Cu distance (3.234 vs 3.269 Å reported here) and DyOOCu dihedral angle (141.2° vs 134.3° in our case), a feeble antiferromagnetic interaction between the ions, in agreement with our findings.

The frequency dependence of the magnetic susceptibility has been

investigated for compounds **2** and **3**, in order to check for slow relaxing magnetization. Compound **3** did not present any out-of-phase magnetic susceptibility signal, irrespective of the static field applied. This may be related to an efficient quantum relaxation mechanism in Er(III) ions with triangular dodecahedron first coordination sphere, which has been reported to disfavour axiality in the magnetic anisotropy by mixing low m_J kets in the ground state Kramers doublet [30]. Compound **2** did not display any slow relaxation with no static magnetic field applied as well, probably because of efficient quantum tunnelling of the magnetization, as previously shown for Dy(III) in a coordination environment with similar geometry [30]. However, the isothermal field scan at 2.5 K showed field-induced slow relaxation, and 2 kOe was chosen as the measurement field, yielding the slowest relaxing magnetic moment without limiting the intensity of the measured signal appreciably (Figure S12). Under this applied field, two sets of temperature and frequency-dependent peaks appear, moving to high frequency upon heating, as reported in the left panel of Fig. 4.

The temperature dependence of the two sets of peaks is strikingly different: while the low frequency one moves to higher frequencies upon heating, the position of the second, higher-frequency, peak stays almost constant, as shown in the right panel of Fig. 4, reporting the relaxation

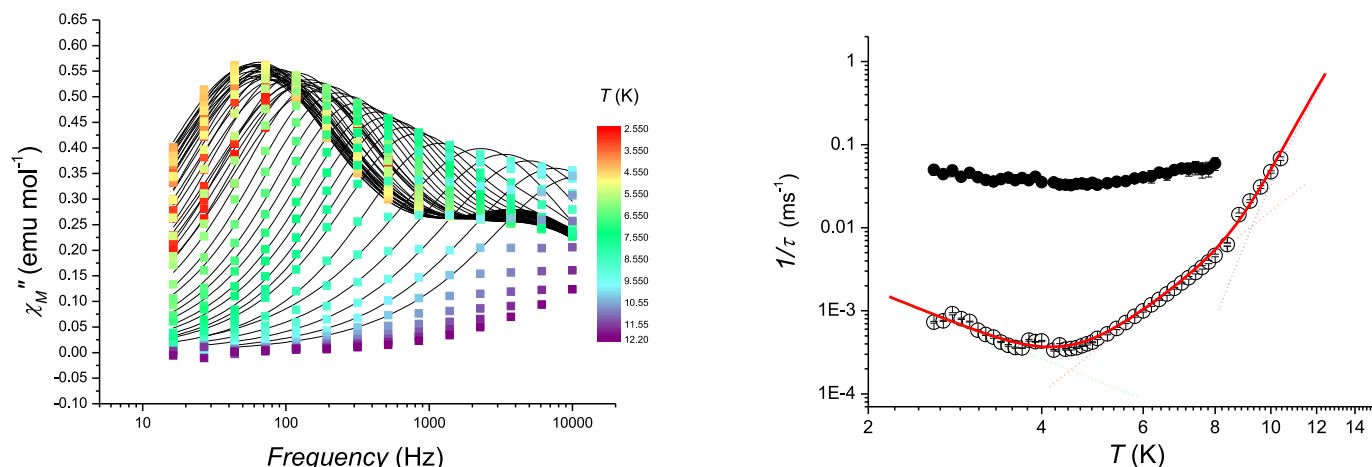


Fig. 4. Left panel: Frequency dependence of the χ''_M of **2**, measured in 2.6 – 12.0 K range. Solid lines are the fitting functions based on the extended Debye model. Right panel: Temperature dependence of the relaxation times of **2**, measured in a 0.2 T applied field. Full points refer to the high frequency, faster relaxation process; the slower one being reported as empty circles. The dotted lines represent the phonon bottleneck (green), Raman (red) and Orbach (blue) isolated contributions to the overall relaxation times, according to the best fitting results using Equation (1). (For interpretation of the references to color in this figure legend, the reader is referred to the web version of this article.)

times τ extracted from the frequency of the maximum of the peaks ($\tau = (2\pi\nu_{\max})^{-1}$). This finding led us to attribute this high-frequency set of peaks as arising from magnetic dipolar interactions in the solid state, as frequently seen for undiluted Dy(III) slow relaxing molecular systems possessing one symmetry inequivalent magnetic ion [34,18]. The temperature dependence of the relaxation times of the lower frequency set of peaks displays a decrease of the relaxation times in the 2.6 – 4.4 K range, which we attribute to the scarcity of phonon modes to activate the spin-phonon relaxation of the magnetic moment (phonon bottleneck effect). Upon further heating, an increase in the relaxation times is found, with a change in slope at about 8.5 K. A best fitting procedure of the temperature dependence of the relaxation times has been realized using a phenomenological approach, previously described by Boskovic and coworkers [35]. In this approach, reported in Equation (1), the phonon bottleneck regime is assumed to be exponentially dependent on temperature, while the region above 4 K has been modelled with a mixed Raman/Orbach mechanism:

$$\frac{1}{\tau} = \frac{B}{T^n} + CT^n + \frac{1}{\tau_0} e^{-\frac{U_{\text{eff}}}{kT}} \quad (1)$$

The best fitting parameters describe a Raman exponent of 5.5(4), while the higher temperature part of the curve, displaying a steeper temperature dependence, yielded an effective barrier to the thermally activated relaxation U_{eff} of 105(26) cm^{-1} . The complete set of best fitting parameters is shown in Table S4. The Raman exponent found here is quite different from the theoretical value of 9 [36], as frequently reported for Dy(III) slow relaxing species, and attributed to the role of optical photons in triggering the relaxation [37,30,2d]. The activation barrier U_{eff} of **2** is higher than the ones previously reported for Dy(III) ions with pseudo-triangular dodecahedron first coordination sphere, featuring a distorted D_{2d} symmetry [30,38]. It must be stressed, however, that in the absence of an experimentally or theoretically estimated energy difference with the excited Kramers doublets, only a tentative attribution of the relaxation mechanisms can be carried out for complex **2**.

2.2. DFT calculations on **1**, **2** and **3**

Further characterizations of the heterometallic $[\text{Ln}(\text{hfac})_3\text{Cu}(\text{acac})_2]$ complexes can be performed by comparing their optimized structures both with experimental X-ray data and with the optimized structures of the two reagents: $[\text{Cu}(\text{acac})_2]$ and $[\text{Ln}(\text{hfac})_3(\text{H}_2\text{O})_2]$ (see Experimental and computational method Section for details). An accurate comparison between the calculated structure for **1** and the X-ray data shows a very good agreement between calculated and experimental values. In more detail, calculated Eu1-O4, Eu1-O7 and Eu1-O8 distances (where O4, O7, O8 are the three oxygen atoms bridging the two metal centres) are in the range 2.482–2.713 Å (exp. 2.438–2.508 Å), and are definitively longer than the other Eu-O distances (2.383–2.418 Å vs exp. 2.336–2.381 Å). The longer calculated Cu-O distance is 2.456 Å (exp. 2.416 Å) for Cu1-O4, (O4 being the bridging hfac oxygen atom) while all the other Cu-O distances are significantly shorter (1.914–1.954 Å vs exp. 1.897–1.966 Å). The Eu1-Cu1 calculated distance is 3.433 Å (exp. 3.306 Å). The calculated values are slightly overestimated with respect to the experimental ones (less than 3.5 %) and this trend can be attributable to the absence of packing effects. Indeed, the heterometallic $[\text{Ln}(\text{hfac})_3\text{Cu}(\text{acac})_2]$ complexes are calculated as isolated molecules and no additional interaction with other molecules is considered even if experimental data shows the formation of a supramolecular dimer.

In addition to the bond lengths, Mulliken's charges and Mulliken's spin population values of the Ln are important parameters for evaluating the bonding properties of the f -block complexes, where the spin polarization is calculated from the difference in α and β spin electronic population of the Ln, thus quantifies the unpaired electrons on the metal. For all heterometallic complexes, the Mulliken's charges of Eu(III), Dy(III) and Er(III) (1.22e, 0.929e and 1.11e for **1**, **2** and **3**, respectively) are

significantly smaller than the formal +3 oxidation states. This suggests a strong ligand-to-metal charge transfer, in line with the literature values for Eu complexes [39]. The net charge of Dy(III) is smaller than that of Eu(III) and Er(III), which means that the charge transfer for the ligands to Dy(III) is greater than in the Eu(III) and Er(III). Similar trends are observed for the $[\text{Ln}(\text{hfac})_3(\text{H}_2\text{O})_2]$ complexes. As regards the second parameter, the spin populations on f -orbitals in the heterometallic complexes are 6.36e, 5.40e and 2.88e for Eu in **1**, Dy in **2** and Er in **3**, respectively while in the $[\text{Ln}(\text{hfac})_3(\text{H}_2\text{O})_2]$ complexes, the calculated values are 6.28e, 4.87e and 2.89e for Eu, Dy and Er. Large deviations of the spin population from formal values (6.00e, 5.00e and 3.00e for Eu, Dy and Er) are indicative of a ligand-to-metal bonding interaction with a higher character of covalency [38,40]. Thus for Dy in **2**, the significative increase in the spin population parameter (5.40e respect to the formal value of 5.00e) indicates that the bonding interactions become less electrostatic in nature with respect to the precursor $[\text{Dy}(\text{hfac})_3(\text{H}_2\text{O})_2]$. On the other hand, the heterometallic complexes **1** and **3** closely look like their lanthanide precursors in this respect.

The variation of the bond strengths from the reagents to the heterometallic complexes can be quantitatively estimated by considering the comparison between their Mayer bond order (MBO) [41]. The MBO is a parameter used to indicate the bonding strength of two adjacent atoms, not necessarily directly connected. The larger the Mayer bond order, the more stable the bond. For the same kind of bond, a correlation can be obtained with the bond order: the longer the bond length, the smaller the bond order. In the $\text{Cu}(\text{acac})_2$, the Cu-O average MBO is 0.627, while for Ln-O_{hfac} in $[\text{Eu}(\text{hfac})_3(\text{H}_2\text{O})_2]$, in $[\text{Dy}(\text{hfac})_3(\text{H}_2\text{O})_2]$ and in $[\text{Er}(\text{hfac})_3(\text{H}_2\text{O})_2]$ are 0.369, 0.417 and 0.424, respectively as expected for stronger bonds for smaller lanthanides.

Outcomes in Table 1 indicate some interesting trends. For all the heterometallic complexes, the MBO values for the Ln-O_{hfac} bond are only slightly affected by the reaction with the $\text{Cu}(\text{acac})_2$ moieties. The only exception is represented by the O4 atom, which directly interacts with the Cu atom. The larger variation, a reduction of the MBO values of 26%, is observed for **1**, with a consequent increment of the MBO value for Cu-O4. On the contrary, **2** and **3** show smaller variations for MBO values for the Ln-O_{hfac} bond, about 10% and 8% respectively in agreement with the lower interaction (MBO less than 0.1) with the Cu-O4. A different trend is observed for the Cu moieties in the heterometallic complexes. In this case, the largest variation of the MBO values is observed for **2** (18%), while for **1** and **3** is about 5% and 8% respectively. However, the most interesting values are the MBO values for copper-lanthanide interactions which are 0.198, 0.492 and below 0.1 for **1**, **2** and **3**, respectively. The high value for **2** indicates a direct relevant interaction between the two metal atoms, even if they are not directly bonded. Similar values for the

Table 1

The MBO values for **1**, **2** and **3** optimized structures. Only values larger than 0.1 are reported. In parenthesis, the average values for Cu-O in $\text{Cu}(\text{acac})_2$ and for Ln-O_{hfac} in $[\text{Ln}(\text{hfac})_3(\text{H}_2\text{O})_2]$. Atom labels are taken from Fig. 1.

	1	2	3
Ln-Cu	0.198	0.492	//
Ln-O1	0.359	0.430	0.444
Ln-O2	0.354	0.429	0.458
Ln-O3	0.358	0.439	0.417
Ln-O4	0.273	0.375	0.389
Ln-O5	0.331	0.419	0.426
Ln-O6	0.331	0.413	0.398
Ln-O7	0.189	0.313	0.180
Ln-O8	0.239	0.366	0.220
Aveg Ln-O _{hfac}	0.334 (0.369)	0.418 (0.417)	0.421 (0.424)
Cu-O4	0.106	//	//
Cu-O7	0.523	0.450	0.495
Cu-O8	0.526	0.403	0.492
Cu-O9	0.676	0.597	0.651
Cu-O10	0.660	0.612	0.679
Aveg Cu-O _{acac}	0.596 (0.627)	0.516 (0.627)	0.579 (0.627)

MBO have been previously calculated for sulphur-sulphur transannular bonding [39]. Indeed, the copper-erbium interaction in **3** is almost negligible. Given the complexity of the molecular orbitals (MOs) in these complexes, a detailed investigation of MOs's compositions is prohibitive, but the MBO has been proven to be a precious tool for considering the bonding and antibonding contributions by the occupied levels in the interaction and finally for clarifying the main bonding contribution to the formation of these heterobimetallic complexes.

3. Conclusions

The $[\text{Ln}(\text{hfac})_3\text{Cu}(\text{acac})_2]$ complexes can be prepared along the 4f series (Ln = Eu, Dy, Er) and are stable in anhydrous conditions. Single crystal diffraction studies show heterometallic dinuclear molecules with three oxygen atoms bridging the two metal centres; one from a hfac and two from acac ligands. The results obtained in this work show that $[\text{Cu}(\text{acac})_2]$ can behave as a Lewis base for $\text{Ln}(\text{hfac})_3$ not exclusively for early-lanthanides fragments. For lanthanum, the molecular complex $[\text{La}(\text{hfac})_3(\text{H}_2\text{O})\text{Cu}(\text{acac})_2]$ is stabilized by the presence of water that is involved in the triple bridge between the two metals. On the other hand, anhydrous conditions are necessary for the synthesis of the dysprosium and erbium *d-f* heterometallic complexes, a result that easily explains previous characterization of products where molecules of $[\text{Cu}(\text{acac})_2]$ and $[\text{RE}(\text{hfac})_3(\text{H}_2\text{O})_2]$ (RE = Dy, Y) are hydrogen bonded in an extended structure. Isothermal magnetization curves point out a feeble antiferromagnetic interaction between Dy(III) and Cu(II) in compound **2**, which showed a field-induced slow relaxation of its magnetic moment, with a significant phonon bottleneck effect. The stronger interaction between the two metal atoms in the copper-dysprosium derivative **2**, with respect to the negligible interaction in **3**, is also supported by the quantum mechanical calculations on the heterometallic complexes.

4. Experimental and computational methods

4.1. Materials and methods.

Anhydrous solvents were purchased from Merck and used as received. $[\text{Ln}(\text{hfac})_3(\text{H}_2\text{O})_2]$ (Ln = Eu, Dy, Er) were prepared according to the literature [42]. FTIR spectra on solid samples were recorded with a Perkin-Elmer "Spectrum One" spectrometer, equipped with an ATR accessory. Elemental analysis (C, H, N) was performed, using an Elementar "vario MICRO cube" instrument, at the Dipartimento di Chimica e Chimica Industriale, Università di Pisa (Italy).

4.2. Synthesis of $[\text{Eu}(\text{hfac})_3\text{Cu}(\text{acac})_2]$, **1**

To a green solution of $[\text{Cu}(\text{acac})_2]$ (0.155 g, 0.59 mmol) in DCE (50 mL), $[\text{Eu}(\text{hfac})_3(\text{H}_2\text{O})_2]$ (0.472 g, 0.58 mmol) was added. The suspension was heated at 60 °C obtaining a cerulean blue solution which was then taken to dryness. The obtained solid was washed with heptane (20 mL) and dried under reduced pressure for 4 h (0.381 g, 62.4 % yield). Elemental analysis calculated for $[\text{Eu}(\text{hfac})_3\text{Cu}(\text{acac})_2]$ ($\text{C}_{25}\text{H}_{17}\text{EuCuF}_{18}\text{O}_{10}$): C 29.0 %, H 1.7 %; found C 29.1 %, H 1.6 %. ATR-IR (1700 – 650 cm^{-1}): 1645 (m), 1585 (w), 1527 (m), 1471 (m), 1399 (w), 1367 (w), 1250 (s), 1201 (s), 1143 (s), 1101 (m), 1022 (w), 937 (w), 805 (m), 741 (w), 659 (m). Single crystals suitable for X-ray analysis were obtained by cooling a heptane solution of **1**. The solid exposed to moisture adsorb water after some days. The process is reversible treating **1** in vacuo at 50 °C over P_4O_{10} . Compound **1** sublimes quantitatively under reduced pressure (10^{-2} mbar) at 110 °C. Crystals of the sublimed product have been recovered from a heptane solution.

4.3. Synthesis of $[\text{Dy}(\text{hfac})_3\text{Cu}(\text{acac})_2]$, **2**

To a green solution of $[\text{Cu}(\text{acac})_2]$ (0.187 g, 0.72 mmol) in DCE (30

mL), $[\text{Dy}(\text{hfac})_3(\text{H}_2\text{O})_2]$ (0.590 g, 0.72 mmol) was added. The suspension was heated at 60 °C obtaining a cerulean blue solution which was then taken to dryness. The obtained solid was washed with heptane (20 mL) and dried under reduced pressure for 4 h over P_4O_{10} (0.600 g, 62.4 % yield). Elemental analysis calculated for $[\text{Dy}(\text{hfac})_3\text{Cu}(\text{acac})_2]$ ($\text{C}_{25}\text{H}_{17}\text{CuDyF}_{18}\text{O}_{10}$): C 28.7 %, H 1.6 %; found C 28.8 %, H 1.6 %. ATR-IR (1700 – 650 cm^{-1}): 1645 (m), 1585 (w), 1527 (m), 1471 (m), 1399 (w), 1367 (w), 1250 (s), 1201 (s), 1143 (s), 1101 (m), 1022 (w), 937 (w), 805 (m), 741 (w), 659 (m). Single crystals suitable for X-ray analysis were obtained by cooling a heptane solution of **2**. The solid exposed to moisture adsorbs water. The process is reversible treating **2** in vacuo at 50 °C over P_4O_{10} .

4.4. Synthesis of $[\text{Er}(\text{hfac})_3\text{Cu}(\text{acac})_2]$, **3**

To a green solution of $[\text{Cu}(\text{acac})_2]$ (0.162 g, 0.62 mmol) in DCE (50 mL), $[\text{Er}(\text{hfac})_3(\text{H}_2\text{O})_2]$ (0.504 g, 0.628 mmol) was added. The suspension was heated at 60 °C obtaining a cerulean blue solution which was then taken to dryness. The obtained solid was washed with heptane (20 mL) and dried under reduced pressure for 4 h over P_4O_{10} (0.329 g, 51.4 % yield). Elemental analysis calculated for $[\text{Er}(\text{hfac})_3\text{Cu}(\text{acac})_2]$ ($\text{C}_{25}\text{H}_{17}\text{ErCuF}_{18}\text{O}_{10}$): C 28.6 %, H 1.8 %; found C 28.8 %, H 1.8 %. ATR-IR (1700 – 650 cm^{-1}): 1645 (m), 1585 (w), 1527 (m), 1471 (m), 1399 (w), 1367 (w), 1250 (s), 1201 (s), 1143 (s), 1101 (m), 1022 (w), 937 (w), 805 (m), 741 (w), 659 (m). Single crystals suitable for X-ray analysis were obtained by cooling a heptane solution of **3**. The solid exposed to moisture adsorb water after few seconds. The process is reversible treating **3** in vacuo at 50 °C over P_4O_{10} . Compound **3** sublimes under reduced pressure (10^{-2} mbar) at 100 °C.

4.5. X-ray diffraction studies

Data were collected using an Oxford Diffraction Gemini E diffractometer, equipped with a 2 K × 2 K EOS CCD area detector and sealed-tube Enhance (Mo) and (Cu) X-ray sources. Mo source was used for compounds **1**, **1a**, **3** and **4** while compound **2** was analyzed with the Cu source. Detector distance has been set at 45 mm. The diffraction intensities have been corrected for Lorentz/polarization effects as well as with respect to absorption. Empirical multi-scan absorption corrections using equivalent reflections have been performed with the scaling algorithm SCALE3 ABSPACK. Data reduction, finalization and cell refinement were carried out through the CrysAlisPro software. Accurate unit cell parameters were obtained by least squares refinement of the angular settings of strongest reflections, chosen from the whole experiment. The structures were solved with Olex2 [43] by using ShelXT structure solution program by Intrinsic Phasing and refined with the ShelXL [44] refinement package using least-squares minimization. In the last cycles of refinement, non-hydrogen atoms were refined anisotropically. Some terminal CF_3 group has been split into two parts the occupancies of which were constrained to sum to 1.0. To better model these disordered groups, SADI restrains for C-F and F...F distances were applied and EADP constrains were applied to selected F atoms. Hydrogen atoms were included in calculated positions, and a riding model was used for their refinement. Table S3 reports crystal data and refinement details for each structure. Cambridge Crystallographic Data Centre (CCDC) numbers 2211377–2211381 contain the supplementary crystallographic data for this paper. These data are provided free of charge by the joint CCDC and Fachinformationszentrum Karlsruhe Access Structures service <https://www.ccdc.ca-m.ac.uk/structures>.

5. Magnetic analysis.

Samples employed for DC (direct current) and AC (alternating current) measurements consisted of pressed microcrystalline powders of compounds **2** and **3**, wrapped in Teflon(TM) tape. The DC magnetic characterization was performed on Quantum Design MPMS (Magnetic

Properties Measurement System) equipment provided with a 7 T magnet. The resulting magnetic data were corrected for the diamagnetic contributions of the ligands calculated from Pascal constants [45], together with those measured for the sample container and the wrapping Teflon tape. The magnetization (M) dependence on the absolute temperature was investigated between 300 and 55 K using a magnetic field (B) of 10 kOe, and between 55 and 2 K with a field of 1 kOe to prevent magnetic saturation. Magnetic susceptibility per mole (χ_M) was then evaluated as $\chi_M = M_M/B$.

Alternating current magnetic susceptibility analyses were performed with a PPMS (Physical Properties Measurement System) platform, also from Quantum Design, with oscillating field frequencies ranging from 10 to 10^4 Hz, using static magnetic fields of zero and 2 kOe. Relaxation times have been determined by least-squares fitting of the isothermal frequency dependence of the out-of-phase molar magnetic susceptibility with an extended Debye model [46].

5.1. Computational details

DFT calculations were carried out by using the Orca suite of programs (version 4.2.0) [47]. The complexes were optimized using the GGA PBE functional [48]; Coulomb and exchange integrals in hybrid calculations were approximated by using the Resolution of Identity approximation with the def2/JK auxiliary basis set [49]. Dispersion corrections were included by adopting Grimme's DFT-D3 method [50]. Each lanthanide is considered in its +3 oxidation state, then Eu(III), Dy(III) and Er(III) have 6, 5 and 3 unpaired electrons, while Cu(II) has one unpaired electron.

Declaration of Competing Interest

The authors declare that they have no known competing financial interests or personal relationships that could have appeared to influence the work reported in this paper.

Data availability

No data was used for the research described in the article.

Acknowledgements

L.L. and S.S. acknowledge the financial support of Pisa University (Fondi di Ateneo 2023). This work is supported by the Università di Pisa under the "PRA – Progetti di Ricerca di Ateneo" (Institutional Research Grants) – Project no. PRA_2022_12 "New challenges of transition metal and lanthanide complexes in the perspective of green chemistry". G.P. gratefully acknowledges FAPERJ for financial support through grants E-26/202.912/2019, SEI-260003/001167/2020, and E-26/010.000978/2019, as well as the support of INCT of Spintronics and Advanced Magnetic Nanostructures (INCT-SpinNanoMag), CNPq 406836/2022-1. The authors are grateful to Professor Luis Ghivelder (Instituto de Física, Universidade Federal do Rio de Janeiro, Brazil) for the access to the magnetic characterization instruments.

Appendix A. Supplementary data

Supplementary data to this article can be found online at <https://doi.org/10.1016/j.ica.2023.121665>.

References

[1] a) M. Sakamoto, K. Manseki, H. Okawa, d-f Heteronuclear complexes: synthesis, structures and physicochemical aspects, *Coord. Chem. Rev.* 219–221 (2001) 379–414, [https://doi.org/10.1016/S0010-8545\(01\)00341-1](https://doi.org/10.1016/S0010-8545(01)00341-1);
b) L. Sorace, C. Benelli, D. Gatteschi, Lanthanides in molecular magnetism: old tools in a new field, *Chem. Soc. Rev.* 40 (2011) 3092–3104, <https://doi.org/10.1039/C0CS00185F>;

c) X. Yang, R.A. Jones, S. Huang, Luminescent 4f and d-4f polynuclear complexes and coordination polymers with flexible salen-type ligands, *Coord. Chem. Rev.* 273–274 (2014) 63–75, <https://doi.org/10.1016/j.ccr.2013.11.012>;
d) K. Liu, W. Shi, P. Cheng, Toward heterometallic single-molecule magnets: Synthetic strategy, structures and properties of 3d–4f discrete complexes, *Coord. Chem. Rev.* 289–290 (2015) 74–122, <https://doi.org/10.1016/j.ccr.2014.10.004>;
e) H.-L. Wang, Z.-H. Zhu, J.-M. Peng, H.-H. Zou, Heterometallic 3d/4f-metal complexes: structure and magnetism, *J. Clust. Sci.* 33 (2022) 1299–1325, <https://doi.org/10.1007/s10876-021-02084-7>;
f) A. Dey, P. Bag, P. Kalita, V. Chandrasekhar, Heterometallic CuII–LnIII complexes: Single molecule magnets and magnetic refrigerants, *Coord. Chem. Rev.* 432 (2021), <https://doi.org/10.1016/j.ccr.2020.213707>, 213707;
g) R.E.P. Winpenny, The structures and magnetic properties of complexes containing 3d- and 4f-metals, *Chem. Soc. Rev.* 27 (1998) 447–452, <https://doi.org/10.1039/A827447Z>;
h) X.-Z. Li, C.-B. Tian, Q.-F. Sun, Coordination-Directed Self-Assembly of Functional Polynuclear Lanthanide Supramolecular Architectures, *Chem. Rev.* 122 (2022) 6374–6458, <https://doi.org/10.1021/acs.chemrev.1c0060>;
i) L.-J. Xu, G.-T. Xu, Z.-N. Chen, Recent advances in lanthanide luminescence with metal-organic chromophores as sensitizers, *Coord. Chem. Rev.* 273–274 (2014) 47–62, <https://doi.org/10.1016/j.ccr.2013.11.021>;
j) M.G.F. Vaz, M. Andruh, Molecule-based magnetic materials constructed from paramagnetic organic ligands and two different metal ions, *Coord. Chem. Rev.* 427 (2021), <https://doi.org/10.1016/j.ccr.2020.213611>, 213611.
[2] a) F. Habib, M. Murugesu, Lessons learned from dinuclear lanthanide nanomagnets, *Chem. Soc. Rev.* 42 (2013) 3278–3288, <https://doi.org/10.1039/c2cs35361j>;
b) R. Sessoli, A.K. Powell, Strategies towards single molecule magnets based on lanthanide ions, *Coord. Chem. Rev.* 253 (2009) 2328–2341, <https://doi.org/10.1016/j.ccr.2008.12.014>;
c) G. Poneti, K. Bernot, L. Bogani, A. Caneschi, R. Sessoli, W. Wernsdorfer, D. Gatteschi, A rational approach to the modulation of the dynamics of the magnetisation in a dysprosium-nitronyl-nitroxide radical complex, *Chem. Commun.* (2007) 1807–1809, <https://doi.org/10.1039/b617898g>;
d) L. Fioravanti, L. Bellucci, L. Armelao, G. Bottaro, F. Marchetti, F. Pineider, G. Poneti, S. Samaritani, L. Labella, Stoichiometrically controlled assembly of lanthanide molecular complexes of the heteroditopic divergent ligand 4'-(4-Pyridyl)-2,2':6,2'-terpyridine N-oxide in hypodentate or bridging coordination modes. structural, magnetic, and photoluminescence studies, *Inorg. Chem.* 61 (2022) 265–278, <https://doi.org/10.1021/acs.inorgchem.1c02809>;
e) L. Bellucci, L. Fioravanti, L. Armelao, G. Bottaro, F. Marchetti, F. Pineider, G. Poneti, S. Samaritani, L. Labella, Size Selectivity in Heterolanthanide Molecular Complexes with a Ditopic Ligand, *Chem. Eur. J.* 29 (2023) e202202823.
[3] a) A. Gaita-Ariño, F. Luis, S. Hill, E. Coronado, Molecular spins for quantum computation, *Nature Chemistry* 11 (2019) 301–309, <https://doi.org/10.1038/s41557-019-0232-y>;
b) G. Aromi, D. Aguila, P. Gamez, F. Luis, O. Roubeau, Design of magnetic coordination complexes for quantum computing, *Chem. Soc. Rev.* 41 (2012) 537–546, <https://doi.org/10.1039/C1CS11151K>.
[4] J.L. Liu, Y.C. Chen, M.L. Tong, Symmetry strategies for high performance lanthanide-based single-molecule magnets, *Chem. Soc. Rev.* 47 (2018) 2431–2453, <https://doi.org/10.1016/j.ccr.2017.11.012>.
[5] J. Long, J.-M. Thibaud, R.A.S. Ferreira, L.D. Carlos, B. Donnadieu, V. Vieu, L. F. Chibotaru, L. Konczewicz, J. Haines, Y. Guari, J. Larionova, A high-temperature molecular ferroelectric Zn/Dy complex exhibiting single-ion-magnet behavior and lanthanide luminescence, *Angew. Chem. Int. Ed.* 54 (2015) 2236–2240, <https://doi.org/10.1002/anie.201410523>.
[6] R.G. Pearson, *Hard and soft acids and bases*, *J. Am. Chem. Soc.* 85 (1962) 3533–3539.
[7] a) M. Andruh, Compartmental Schiff-base ligands—a rich library of tectons in designing magnetic and luminescent materials, *Chem. Commun.* 47 (2011) 3025–3042, <https://doi.org/10.1039/c0cc04506g>;
b) L. Armelao, D. Belli Dell'Amico, G. Bottaro, L. Bellucci, L. Labella, F. Marchetti, C.A. Mattei, F. Mian, F. Pineider, G. Poneti, S. Samaritani, 1D hetero-bimetallic regularly alternated 4f–3d coordination polymers based on N-oxide-4,4'-bipyridine (bipyMO) as a linker: photoluminescence and magnetic properties, *Dalton Trans.* 47 (2018) 8337–8345, <https://doi.org/10.1039/c8dt00880a>;
c) L. Bellucci, G. Bottaro, L. Labella, V. Causin, F. Marchetti, S. Samaritani, D. Belli Dell'Amico, L. Armelao, Composition—thermometric properties correlations in homodinuclear Eu3+ luminescent complexes, *Inorg. Chem.* 59 (2020) 18156–18167, <https://doi.org/10.1021/acs.inorgchem.0c02611>.
[8] a) V. Chandrasekhar, T. Senapati, A. Dey, S. Das, M. Kalisz, R. Clérac, Cyclo- and Carbophosphazene-Supported Ligands for the Assembly of Heterometallic (Cu2+/Ca2+, Cu2+/Dy3+, Cu2+/Tb3+) Complexes: Synthesis, Structure, and Magnetism, *Inorg. Chem.* 51 (2012) 2031–2038, <https://doi.org/10.1021/ic201463g>;
b) F. He, M.-L. Tong, X.-M. Chen, Synthesis, Structures, and Magnetic Properties of Heteronuclear Cu(II)–Ln(III) (Ln = La, Gd, or Tb) Complexes, *Inorg. Chem.* 44 (2005) 8285–8292, <https://doi.org/10.1021/ic0507159>;
c) T. Ishida, R. Watanabe, K. Fujiwara, A. Okazawa, N. Kojima, G. Tanaka, S. Yoshii, H. Nojiri, Exchange coupling in TbCu and DyCu single-molecule magnets and related lanthanide and vanadium analogs, *Dalton Trans.* 41 (2012) 13609–13619, <https://doi.org/10.1039/C2DT31169K>;
d) J.-P. Costes, F. Dahan, W. Wernsdorfer, Heterodinuclear Cu–Tb Single-molecule magnet, *Inorg. Chem.* 45 (2006) 5–7, <https://doi.org/10.1021/ic050563h>;

- e) M. Dolai, M. Ali, J. Titiš, R. Boča, Cu(II)–Dy(III) and Co(III)–Dy(III) based single molecule magnets with multiple slow magnetic relaxation processes in the Cu(II)–Dy(III) complex, *Dalton Trans.* 44 (2015) 13242–13249, <https://doi.org/10.1039/C5DT00960j>;
- f) A. Jana, S. Majumder, L. Carrella, M. Nayak, T. Weyhermueller, S. Dutta, D. Schollmeyer, E. Rentschler, R. Koner, S. Mohanta, Syntheses, structures, and magnetic properties of diphenoxo-bridged Cu(II)Ln(III) and Ni(II)(Low-Spin)Ln(III) compounds derived from a compartmental ligand (Ln = Ce–Yb), *Inorg. Chem.* 49 (2010) 9012–9025, <https://doi.org/10.1021/ic101445n>;
- g) T. Kajiwara, M. Nakano, K. Takahashi, S. Takaishi, M. Yamashita, Structural design of easy-axis magnetic anisotropy and determination of anisotropic parameters of Ln(III)–Cu(II) single-molecule magnets, *Chem. Eur. J.* 17 (2011) 196–205, <https://doi.org/10.1002/chem.201002434>;
- h) T. Kajiwara, M. Nakano, S. Takaishi, M. Yamashita, Coordination-Tuned Single-Molecule-Magnet Behavior of Tb(III)–Cu(II) Dinuclear Systems, *Inorg. Chem.* 47 (2008) 8604–8606, <https://doi.org/10.1021/ic8013656>;
- i) J.-J. Kong, J.-C. Zhang, Y.-X. Jiang, J.-X. Tao, W.-Y. Wang, X.-C. Huang, Two-dimensional heterometallic Cu(II)Ln(III) (Ln = Tb and Dy) coordination polymers bridged by dicyanamides showing slow magnetic relaxation behaviour, *CrystEngComm* 21 (2019) 5145–5151, <https://doi.org/10.1039/C9CE00673G>;
- l) S. Maity, P. Bhunia, K. Ichihashi, T. Ishida, A. Ghosh, SMM behaviour of heterometallic dinuclear Cu(II) Ln(III) (Ln = Tb and Dy) complexes derived from N2O3 donor unsymmetrical ligands, *New J. Chem.* 44 (2020) 6197–6205, <https://doi.org/10.1039/D0NJ00193G>;
- m) T. Ueno, T. Fujinami, N. Matsumoto, M. Furusawa, R. Irie, N. Re, T. Kanetomo, T. Ishida, Y. Sunatsuki, Circular and chainlike Copper(II)–lanthanide(III) complexes generated by assembly reactions of racemic and chiral copper(II) cross-linking ligand complexes with Ln(III)(NO₃)₃·6H₂O (Ln(III) = Gd(III), Tb(III), Dy(III)), *Inorg. Chem.* 56 (2017) 1679–1695, <https://doi.org/10.1021/acs.inorgchem.6b02668>;
- n) J.-W. Zhang, X.-M. Kan, B.-Q. Liu, G.-C. Liu, A.-X. Tian, X.-L. Wang, Systematic investigation of reaction-time dependence of three series of copper–lanthanide/lanthanide coordination polymers: syntheses, structures, photoluminescence, and magnetism, *Chem. Eur. J.* 21 (2015) 16219–16228, <https://doi.org/10.1002/chem.201502203>.
- [9] K. Binnemans, Rare-Earth Beta-Diketonates, *Handb. Phys. Chem. Rare Earths* 35 (2005) 107–272, [https://doi.org/10.1016/S0168-1273\(05\)35003-3](https://doi.org/10.1016/S0168-1273(05)35003-3).
- [10] a) G. Cosquer, F. Pointillart, Y. Le Gal, S. Golhen, O. Cador, L. Ouahab, Ferromagnetic versus antiferromagnetic exchange interactions in tetrathiafulvalene-based 3d/4f heterobimetallic complexes, *Chem. Eur. J.* 17 (2011) 12502–12511, <https://doi.org/10.1002/chem.201100360>;
- b) N.P. Kuz'mina, I.P. Malkerova, A.S. Alikhanyan, A.N. Gleizes, The use of 3d-metal complexes as ligands to prepare volatile 4f–3d heterobimetallic complexes, *J. Alloys Compd.* 374 (2004) 315–319, <https://doi.org/10.1016/j.jallcom.2003.11.098>;
- c) C. Benelli, A. Caneschi, D. Gatteschi, O. Guillou, L. Pardi, Synthesis, crystal structure, and magnetic properties of tetranuclear complexes containing exchange-coupled Ln₂Cu₂ (Ln = Gd, Dy) species, *Inorg. Chem.* 29 (1990) 1750–1755, <https://doi.org/10.1021/ic00334a031>;
- d) R. Jia, H.-F. Li, P. Chen, T. Gao, W.-B. Sun, G.-M. Li, P.-F. Yan, Synthesis, structure, and tunable white light emission of heteronuclear Zn₂Ln₂ arrays using a zinc complex as ligand, *CrystEngComm* 18 (2016) 917–923, <https://doi.org/10.1039/C5CE02228B>;
- e) L. Chen, S.R. Breeze, R.J. Rousseau, S. Wang, L.K. Thompson, Polynuclear Copper–Lanthanide Complexes with Amino Alcohol Ligands. Syntheses, Structures, and Magnetic and Spectroscopic Studies of Cu(II)(bdmmp)₂(H₂O), Pr(III)Cu(II)(bdmmp)(bdmmpH)(μ-OH)(hfacac)₃, [La(III)Cu(II)(bdmmp)(bdmmpH)(μ-OH)(O₂CCF₃)₃]₂, and Cu(II)(bdmmp)₂(μ₄-O)(O₂CCF₃)₄, (bdmmpH = 2,6-Bis[(dimethylamino)methyl]-4-methylphenol; hfacac = Hexafluoroacetylacetonato), *Inorg. Chem.* 34 (1995) 454–465, <https://doi.org/10.1021/ic00106a007>.
- [11] a) I. Ramade, O. Kahn, Y. Jeannin, F. Robert, Design and Magnetic Properties of a Magnetically Isolated Gd(III)Cu(II) Pair. Crystal Structures of [Gd(hfa)₃Cu(salen)], [Y(hfa)₃Cu(salen)], [Gd(hfa)₃Cu(salen)(Meim)], and [La(hfa)₃(H₂O)Cu(salen)] [hfa = Hexafluoroacetylacetonato, salen = N, N'-Ethylenebis(salicylideneaminato), Meim = 1-Methylimidazole], *Inorg. Chem.* 36 (1997) 930–936, <https://doi.org/10.1021/ic9607595>;
- b) A.N. Gleizes, M. Julve, N.P. Kuz'mina, A.S. Alikhanyan, F. Lloret, I. P. Malkerova, J.L. Sanz, F. Senocq, Heterobimetallic d₂f metal complexes as potential single-source precursors for MOCVD: structure and thermodynamic study of the sublimation of [Ni(salen)Ln(hfa)₃], Ln = Y, Gd, *Eur. J. Inorg. Chem.* (1998) 1169–1174, [https://doi.org/10.1002/\(SICI\)1099-0682\(199808\)1998:8<1169::AID-EJIC1169>3.0.CO;2-Q](https://doi.org/10.1002/(SICI)1099-0682(199808)1998:8<1169::AID-EJIC1169>3.0.CO;2-Q);
- c) F. Pointillart, K. Bernot, Determination of the nature of exchange interactions in the 3d–4f magnetic chain {[Cu(salen)Pr(hfac)₃]₂(L)}_n (L = 4,4'-Bipyridine, Pyrazine), *Eur. J. Inorg. Chem.* (2010) 952–964, <https://doi.org/10.1002/ejic.200901012>.
- [12] a) M. Sasaki, H. Horiuchi, M. Kumagai, M. Sakamoto, H. Sakiyama, Y. Nishida, Y. Sadaoka, M. Ohba, H. Okawa, A novel discrete d-f heterobimetallic complex designed from tetrahedrally distorted [Cu(salabza)](H₂salabza): N, N'-Bis(salicylidene)-2-aminobenzylamine and [Gd(hfac)₃], *Chem. Lett.* (1998) 911–912, <https://doi.org/10.1246/cl.1998.911>;
- b) M. Sasaki, K. Manseki, H. Horiuchi, M. Kumagai, M. Sakamoto, H. Sakiyama, Y. Nishida, M. Saki, Y. Sadaoka, M. Ohba, H. Okawa, Synthesis, structure, and magnetic properties of discrete d-f heterodinuclear complexes designed from tetrahedrally distorted [Cu(salabza)](H₂salabza) = N, N'-bis(salicylidene)-2-aminobenzylamine and [Ln(hfac)₃] (Hfacac = 1,1,1,5,5,5-hexafluoroacetylacetonato, Ln = Gd or Lu), *J. Chem. Soc., Dalton Trans.* (2000) 259–263, <https://doi.org/10.1039/A907423F>;
- c) M. Ryazanov, V. Nikiforov, F. Lloret, M. Julve, N.P. Kuz'mina, A. Gleizes, Magnetically Isolated Cu(II)Gd(III) Pairs in the Series [Cu(acacen)Gd(pta)₃], [Cu(acacen)Gd(hfa)₃], [Cu(salen)Gd(pta)₃], and [Cu(salen)Gd(hfa)₃], [acacen = N, N'-Ethylenebis(acetylacetonimate(–)), salen = N, N'-Ethylenebis(salicylideneiminato(–)), hfa = 1,1,1,5,5,5-Hexafluoropentane-2,4-dionate(–), pta = 1,1,1-Trifluoro-5,5-dimethylhexane-2,4-dionate(–)], *Inorg. Chem.* 41 (2002) 1816–1823, <https://doi.org/10.1021/ic00110777>;
- d) G. Cosquer, F. Pointillart, B. Le Guennic, Y. Le Gal, S. Golhen, O. Cador, L. Ouahab, 3d4f Heterobimetallic Dinuclear and Tetranuclear Complexes Involving Tetrathiafulvalene as Ligands: X-ray Structures and Magnetic and Photophysical Investigations, *Inorg. Chem.* 51 (2012) 8488–8501, <https://doi.org/10.1021/ic3010689>;
- e) C. Brewer, G. Brewer, W.R. Scheidt, M. Shang, E.E. Carpenter, Synthesis and structural and magnetic characterization of discrete phenolato and imidazole bridged Gd(III)–M(II) [M = Cu, Ni] dinuclear complexes, *Inorg. Chim. Acta* 313 (2001) 65–70, [https://doi.org/10.1016/S0020-1693\(00\)00354-6](https://doi.org/10.1016/S0020-1693(00)00354-6);
- f) M. Ohba, N. Ohtsubo, T. Shiga, M. Sakamoto, H. Okawa, Synthesis, structure and magnetic properties of a linear Cu(II)Cu(II)Gd(III) complex, *Polyhedron* 22 (2003) 1905–1910, [https://doi.org/10.1016/S0277-5387\(03\)00145-1](https://doi.org/10.1016/S0277-5387(03)00145-1).
- [13] A. Benicini, C. Benelli, A. Caneschi, R.L. Carlini, A. Dei, D. Gatteschi, Crystal and molecular structure of and magnetic coupling in two complexes containing gadolinium(III) and copper(II) ions, *J. Am. Chem. Soc.* 107 (1985) 8128–8136, <https://doi.org/10.1021/ja00312a054>.
- [14] a) J.A. Peters, K. Djanashvili, C.F.G.C. Geraldes, C. Platas-Iglesias, The chemical consequences of the gradual decrease of the ionic radius along the Ln-series, *Coord. Chem. Rev.* 406 (2020) j.ccr.2019.213146;
- b) G.S. Silva, J.D.L. Dutra, N.B. da Costa Jr., S. Alves Jr., R.O. Freire, Lanthanide contraction in lanthanide organic frameworks: A theoretical and experimental study, *J. Phys. Chem. A* 124 (2020) 7678–7684, <https://doi.org/10.1021/acs.jpca.0c05065>;
- c) M. Seitz, A.G. Oliver, K.N. Raymond, The lanthanide contraction revisited, *J. Am. Chem. Soc.* 129 (2007) 11153–11160, <https://doi.org/10.1021/ja072750f>;
- d) U. Baisch, D. Belli Dell'Amico, F. Calderazzo, L. Labella, F. Marchetti, A. Merigo, N,N-dialkylcarbamato lanthanide complexes, a series of isotypical coordination compounds, *Eur. J. Inorg. Chem.* (2004) 1219–1224, <https://doi.org/10.1002/ejic.200300649>.
- [15] a) S.A. Cotton, P.R. Raithby, Systematics and surprises in lanthanide coordination chemistry, *Coord. Chem. Rev.* 340 (2017) 220–231, <https://doi.org/10.1016/j.ccr.2017.01.011>;
- b) U. Baisch, D. Belli Dell'Amico, F. Calderazzo, R. Conti, L. Labella, F. Marchetti, E.A. Quadrelli, The mononuclear and dinuclear dimethoxyethane adducts of lanthanide trichlorides [LnCl₃(DME)₂]_n, n = 1 or 2, fundamental starting materials in lanthanide chemistry: preparation and structures, *Inorg. Chim. Acta* 357 (2004) 1538–1548, <https://doi.org/10.1016/j.jica.2003.11.011>.
- [16] A.Y. Rogachev, A.V. Mironov, A.V. Nemukhin, Experimental and theoretical studies of the products of reaction between Ln(hfa)₃ and Cu(acac)₂ (Ln = La, Y; acac = acetylacetonate, hfa = hexafluoroacetylacetonate), *J. Mol. Struct.* 831 (2007) 46–54, <https://doi.org/10.1016/j.molstruc.2006.07.018>.
- [17] Y.S. Jung, J.H. Lee, K. Park, S.-I. Cho, S.-J. Kang, The self-assembly of Y(hfa)₃(H₂O)₂ with Cu(acac)₂, *Bull. Korean Chem. Soc.* 19 (1998) 699–702.
- [18] X.-L. Li, J. Li, A. Wang, C.-M. Liu, M. Cui, Y.-Q. Zhang, Observation of field-induced single-ion magnet behavior in a mononuclear Dy(III) complex by co-crystallization of a square-planar Cu(II) complex, *Inorg. Chim. Acta* 510 (2020), 119718, <https://doi.org/10.1016/j.ica.2020.119718>.
- [19] N.P. Kuz'mina, M.V. Ryazanov, V.Z. Ketsko, A.N. Gleizes, *Russ. J. Inorg. Chem.* 47 (2002) 26 [Zh. Neorg.Khim. 47, 30].
- [20] a) C.M. Lieberman, A.S. Filatov, Z. Wei, A.Y. Rogachev, A.M. Abakumov, E. V. Dikarev, Mixed-valent, heteroleptic homometallic diketonates as templates for the design of volatile heterometallic precursors, *Chem. Sci.* 6 (2015) 2835–2842, <https://doi.org/10.1039/c4sc04002c>;
- b) S. Mishra, S. Daniele, Metal–organic derivatives with fluorinated ligands as precursors for inorganic nanomaterials, *Chem. Rev.* 115 (2015) 8379–8448, <https://doi.org/10.1021/cr400637c>;
- c) G.G. Condorelli, G. Malandrino, I.L. Fragalà, Engineering of molecular architectures of β-diketonate precursors toward new advanced materials, *Coord. Chem. Rev.* 251 (2007) 1931–1950, <https://doi.org/10.1016/j.ccr.2007.04.016>;
- d) N.P. Kuz'mina, I.P. Malkerova, A.S. Alikhanyan, A.N. Gleizes, The use of 3d-metal complexes as ligands to prepare volatile 4f–3d heterobimetallic complexes, *J. Alloys Compd.* 374 (2004) 315–319, <https://doi.org/10.1016/j.jallcom.2003.11.098>.
- [21] L.F. Lindoy, H.C. Lip, H.W. Louie, M.G.B. Drew, M.J. Hudson, Interaction of lanthanide shift reagents with co-ordination complexes; direct observation of nuclear magnetic resonance signals for free and complexed tris(pentane-2,4-dionato)cobalt(III) at ambient temperature, and X-ray crystal and molecular structure, *J. Chem. Soc. Chem. Commun.* (1977) 778–780, <https://doi.org/10.1039/c39770000778>.
- [22] a) N. Kameta, H. Imura, K. Ohashi, T. Aoyama, Equilibrium and spectroscopic studies on the complexation of tris(1-(2-thienyl)-4,4,4-trifluoro-1,3-butanedionato)lanthanoids(III) with tris(2,4-pentanedionato)cobalt(III) as complex ligand, *Inorg. Chem. Commun.* 2 (1999) 124–127, [https://doi.org/10.1016/S1387-7003\(99\)00027-1](https://doi.org/10.1016/S1387-7003(99)00027-1);
- b) N. Kameta, H. Imura, K. Ohashi, T. Aoyama, Stability constants of inner- and outer-sphere complexes of hydrated tris(1-(2-thienyl)-4,4,4-trifluoro-1,3-butanedionato)lanthanide(III) with tris(2,4-pentanedionato)cobalt(III),

- Polyhedron 21 (2002) 805–810, [https://doi.org/10.1016/S0277-5387\(02\)00858-6](https://doi.org/10.1016/S0277-5387(02)00858-6).
- [23] A. Øvre, M. Vinum, M. Kern, J. van Slageren, J. Bendix, M. Perfetti, Chiral, heterometallic lanthanide-transition metal complexes by design, *Inorganics* 6 (2018) 72–81, <https://doi.org/10.3390/inorganics6030072>.
- [24] L. Bellucci, L. Babetto, G. Bottaro, S. Carlotto, L. Labella, E. Gallo, F. Marchetti, S. Samaritani, L. Armelao, Competing excitation paths in Luminescent Heterobimetallic Ln-Al complexes: unravelling interactions via experimental and theoretical investigations, *iScience* 26 (2023), <https://doi.org/10.1016/j.isci.2023.106614>, 106614.
- [25] D. Casanova, M. Llundell, P. Alemany, S. Alvarez, The rich stereochemistry of eight-vertex polyhedra: a continuous shape measures study, *Chem. Eur. J.* 11 (2005) 1479–1494, <https://doi.org/10.1002/chem.200400799>.
- [26] a) A.A. Patrascu, M. Briganti, S. Soriano, S. Calancea, R.A. Allão Cassaro, F. Totti, M.G.F. Vaz, M. Andruh, SMM Behavior Tuned by an Exchange Coupling LEGO Approach for Chimeric Compounds: First 2p–3d–4f Heterotriscipin Complexes with Different Metal Ions Bridged by One Aminoxyl Group, *Inorg. Chem.* 58 (2019) 13090–13101, <https://doi.org/10.1021/acs.inorgchem.9b01998>;
b) J. Zhang, C. Li, J. Wang, M. Zhu, L. Li, Slow Magnetic Relaxation Behavior in Rare Ln–Cu–Ln Linear Trinuclear Complexes, *Eur. J. Inorg. Chem.* (2016) 1383–1388, <https://doi.org/10.1002/ejic.201501388>;
c) C. Aronica, G. Chastanet, G. Pilet, B. Le Guennic, V. Robert, W. Wernsdorfer, D. Luneau, Cubane Variations: Syntheses, Structures, and Magnetic Property Analyses of Lanthanide(III)–Copper(II) Architectures with Controlled Nuclearities, *Inorg. Chem.* 46 (2007) 6108–6119, <https://doi.org/10.1021/ic700645q>.
- [27] G. Trucollo, Z. Tessari, J. Tessarolo, S. Quici, L. Armelao, M. Rancan, A Cu(II) Metallocycle for the Reversible Self-Assembly of Coordination-Driven Polyrotaxane-like Architectures, *Dalton Trans.* 47 (2018) 12079–12084, <https://doi.org/10.1039/C8DT02693A>.
- [28] a) I.A. Baidina, P.A. Stabnikov, I.K. Igumenov, S.V. Borisov, Crystal and molecular structure of copper(II) acetylacetonate hexafluoroacetylacetonate, *Koordinatsionnaia khimiia* 10 (1984) 1699–1705;
b) P.C. Le Brun, W.D. Lyon, H.A. Kuska, Effects of mixed-ligand complexation on the geometry of copper(II) complexes. X-ray study of (hexafluoroacetylacetonato) (acetylacetonato) copper(II), *Inorg. Chem.* 25 (1986) 3106–3108, <https://doi.org/10.1021/ic00237a039>.
- [29] N.P. Kuzmina, G.N. Kupriyana, S.I. Troyanov, Crystal structure and vacuum sublimation of the product of reaction of yttrium hexafluoroacetylacetonate and copper acetylacetonate $[Y(hfa)_3(H_2O)_2Cu(acac)_2]$, *Russ. J. Coord. Chem.* 26 (2000) 367–372. Translation of *Koordinatsionnaia Khimiya*.
- [30] N. Monni, J.J. Baldoví, V. García-López, M. Oggianu, E. Cadoni, F. Quochi, M. Clemente-León, M.L. Mercuri, E. Coronado, Reversible tuning of luminescence and magnetism in a structurally flexible erbium–anilato MOF, *Chem. Sci.* 13 (2022) 7419–7428, <https://doi.org/10.1039/d2sc00769j>.
- [31] a) F. Mori, T. Nyui, T. Ishida, T. Nogami, K.-Y. Choi, H. Nojiri, Oximate-bridged trinuclear Dy–Cu–Dy complex behaving as a single-molecule magnet and its mechanistic investigation, *J. Am. Chem. Soc.* 128 (2006) 1440–1441, <https://doi.org/10.1021/ja057183f>;
b) A. Okazawa, T. Nogami, H. Nojiri, T. Ishida, Ferromagnetic Dy–Ni and antiferromagnetic Dy–Cu couplings in single-molecule magnets $[Dy_2Ni]$ and $[Dy_2Cu]$, *Inorg. Chem.* 47 (2008) 9763–9765, <https://doi.org/10.1021/ic801686z>.
- [32] a) S. Ueki, T. Ishida, T. Nogami, K.-Y. Choi, H. Nojiri, Quantum tunneling of magnetization via well-defined Dy–Cu exchange coupling in a ferrimagnetic high-spin $[Dy_4Cu]$ single-molecule magnet, *Chem. Phys. Lett.* 440 (2007) 263–267, <https://doi.org/10.1016/j.cplett.2007.04.063>;
b) S. Ueki, A. Okazawa, T. Ishida, T. Nogami, H. Nojiri, Tetranuclear heterometallic cycle Dy_2Cu_2 and the corresponding polymer showing slow relaxation of magnetization reorientation, *Polyhedron* 26 (2007) 1970–1976, <https://doi.org/10.1016/j.poly.2006.09.048>.
- [33] a) J.-P. Costes, F. Dahan, A. Dupuis, J.-P. Laurent, Nature of the Magnetic interaction in the (Cu_2^+, Ln_3^+) pairs: an empirical approach based on the comparison between homologous (Cu_2^+, Ln_3^+) and (Ni_2^+LS, Ln_3^+) complexes, *Chem. Eur. J.* 4 (1998) 1616–1620, [https://doi.org/10.1002/\(SICI\)1521-3765\(19980904\)4:9<1616::AID-CHEM1616>3.0.CO;2-A](https://doi.org/10.1002/(SICI)1521-3765(19980904)4:9<1616::AID-CHEM1616>3.0.CO;2-A);
b) M. Sakamoto, M. Hashimura, K. Matsuki, N. Matsumoto, K. Inoue, H. Okawa, Ferromagnetic spin-coupling between gadolinium(III) and copper(II) ions in discrete binuclear Gd(III)–Cu(II) complexes, *Bull. Chem. Soc. Jpn.* 64 (1991) 3639–3641, <https://doi.org/10.1021/ic9811998>;
c) J.-P. Costes, S. Shovab, W. Wernsdorfer, Tetranuclear $[Cu–Ln]_2$ single molecule magnets: synthesis, structural and magnetic studies, *Dalton Trans.* (2008) 1843–1849, <https://doi.org/10.1039/b716098d>;
d) T. Kajiwara, M. Nakano, K. Takahashi, S. Takaishi, M. Yamashita, Structural design of easy-axis magnetic anisotropy and determination of anisotropic parameters of $LnIII CuII$ single-molecule magnets, *Chem. Eur. J.* 17 (2011) 196–205, <https://doi.org/10.1002/chem.201002434>.
- [34] L. Bellucci, L. Labella, F. Marchetti, F. Pineider, G. Poneti, S. Samaritani, Magnetic relaxation in dysprosium and terbium 1D-zigzag coordination chains having only 4,4'-bipyridine as connector, *Inorg. Chim. Acta* 516 (2021), 120165, <https://doi.org/10.1016/j.ica.2020.120165>.
- [35] E. Rousset, M. Piccardo, M.-E. Boulon, R.W. Gable, A. Soncini, L. Sorace, C. Boskovic, Slow magnetic relaxation in lanthanoid crown ether complexes: interplay of Raman and anomalous phonon bottleneck processes, *Chem. Eur. J.* 24 (2018) 14768–14785, <https://doi.org/10.1002/chem.201702779>.
- [36] A. Abragam, B. Bleaney, *Electron Paramagnetic Resonance of Transition Ions*, Oxford University Press, Oxford, 1970.
- [37] K.N. Shrivastava, Theory of spin-lattice relaxation, *Phys. Status Solidi B* 117 (1983) 437–458, <https://doi.org/10.1002/psb.2221170202>.
- [38] a) A.-Q. Xue, Y.-Y. Liu, J.-X. Li, Y. Zhang, Y.-S. Meng, W.-H. Zhu, Y.-Q. Zhang, H.-L. Sun, F. Wang, G.-X. Qiu, L.-Y. Liang, X. Wang, S. Gao, The differential magnetic relaxation behaviours of slightly distorted triangular dodecahedral dysprosium analogues in a type of cyano-bridged 3d–4f zig-zag chain compounds, *Dalton Trans.* 49 (2020) 6867–6875, <https://doi.org/10.1039/D0DT00990C>;
b) S. Roy, J. Du, E. Manu Manohar, L. Sun, N. Ahmed, A. Dey, S. Das, Mononuclear Lanthanide Complexes in Triangular Dodecahedron Geometry: Manifestation of Single Ion Magnet Behavior for Dy(III) Analogue, *Cryst. Growth Des.* 23 (2023) 1066–1075, <https://doi.org/10.1021/acs.cgd.2c01226>.
- [39] Y. Fan, Y. Li, X. Shu, R. Wu, S. Chen, Y. Jin, C. Xu, J. Chen, C. Huang, C. Xia, Complexation and separation of trivalent actinides and lanthanides by a novel DGA derived from macrocyclic crown ether: synthesis, extraction, and spectroscopic and density functional theory studies, *ACS Omega* 6 (2021) 2156–2166, <https://doi.org/10.1021/acsomega.0c05317>.
- [40] T. Kimura, M. Kaneko, M. Watanabe, S. Miyashita, S. Nakashima, Computational chemical analysis of $Eu(III)$ and $Am(III)$ complexes with pnictogen-donor ligands using DFT calculations, *Dalton Trans.* 47 (2018) 14924–14931, <https://doi.org/10.1039/c8dt01973h>.
- [41] A.J. Bridgeman, G. Cavigliasso, L.R. Ireland, J. Rothery, The Mayer bond order as a tool in inorganic chemistry, *J. Chem. Soc., Dalton Trans.* (2001) 2095–2108, <https://doi.org/10.1039/b102094n>.
- [42] S.J. Lyle, A.D. Witts, *Inorg. Chim. Acta* 5 (1971) 481–484, [https://doi.org/10.1016/S0020-1693\(00\)95970-X](https://doi.org/10.1016/S0020-1693(00)95970-X).
- [43] O.V. Dolomanov, L.J. Bourhis, R.J. Gildea, J.A.K. Howard, H. Puschmann, OLEX2: A complete structure solution, refinement and analysis program, *J. Appl. Crystallogr.* 42 (2009) 339–341, <https://doi.org/10.1107/S0021889808042726>.
- [44] G.M. Sheldrick, Crystal structure refinement with SHELXL, *Acta Crystallogr. Sect. C Struct. Chem.* 71 (2015) 3–8, <https://doi.org/10.1107/S2053229614024218>.
- [45] G.A. Bain, J.F. Berry, Diamagnetic corrections and Pascal's constants, *J. Chem. Educ.* 85 (2008) 532–534, <https://doi.org/10.1021/ed085p532>.
- [46] D. Gatteschi, R. Sessoli, J. Villain, *Molecular Nanomagnets*, Oxford University Press, Oxford, 2006.
- [47] F. Neese, Software update: The ORCA program system, *Version 4.0*. Wiley Interdiscip. Rev. Comput. Mol. Sci. 8 (2018) 4–9.
- [48] a) J.P. Perdew, Y. Wang, Accurate and simple analytic representation of the electron-gas correlation energy, *Phys. Rev. B* 45 (1992) 13244–13249, <https://doi.org/10.1103/PhysRevB.45.13244>;
b) J.P. Perdew, K. Burke, M. Ernzerhof, Generalized Gradient Approximation Made Simple, *Phys. Rev. Lett.* 77 (18) (1996) 3865–3868, <https://doi.org/10.1103/PhysRevLett.77.3865>.
- [49] F. Weigend, Hartree-Fock exchange fitting basis sets for H to Rn, *J. Comput. Chem.* 29 (2007) 167–175, <https://doi.org/10.1002/jcc.20702>.
- [50] T.A. Wesolowski, Comment on “Accurate frozen-density embedding potentials as a first step towards a subsystem description of covalent bonds”, *J. Chem. Phys.* 132 (2010), 164101 <https://doi.org/10.1063/1.3609108>.